Performance Analysis for DM-RS Mapping in a High Speed Train System

Jihyung Kim(✉), Juho Park, Junghoon Lee, and JunHwan Lee

Electronics and Telecommunications Research Institute, Daejeon, Korea
savant21@etri.re.kr

Abstract. In this paper, we analyze performances for BLER and spectral efficiency in a high speed train (HST) system. The HST scenario is one of 5G mobile communication services. The performance analysis is evaluated in accordance with DM-RS mapping for channel estimation. DM-RS mapping is associated with high Doppler and frequency flat channel properties of the HST scenario. The performance results show that DM-RS in new radio (NR) satisfies the performance requirement of HST in ITU-R and a modified DM-RS mapping can be more efficient in HST channel properties.

Keywords: 5G NR · High speed train · DM-RS · Frequency selectivity

1 Introduction

1.1 A Subsection Sample

5G mobile communications should satisfy requirements to support various service scenarios, including high transmission speeds for enhanced mobile broadband (eMBB) service, short transfer delays with reliability for ultra reliable and low latency communication (URLLC) service, and large terminal connectivity for massive machine type communication (mMTC) service [1]. ITU-R working party (WP) 5D suggests specific technical performance requirements such as peak data rate, average spectral efficiency, reliability, and mobility [2]. In addition, it suggests guidelines for evaluation of radio interface technologies such as system and link level parameters, channel model, and network layout [3].

In order to address these requirements, 3rd Generation Partnership Project (3GPP) studied new wireless access technology called new radio (NR) [4]. Based on these studies, it is currently developing technical specifications [5–10]. NR does not have backward compatibility with long term evolution (LTE) and maintains forward compatibility for supporting various services in the future. One of

This work was supported by Institute for Information & communications Technology Promotion (IITP) grant funded by the Korea government (MSIT) (No. 2017-0-01973 (Korea-Japan) International collaboration of 5G mmWave based Wireless Channel Characteristic and Performance Evaluation in High Mobility Environments).

O. Galinina et al. (Eds.): NEW2AN 2018/ruSMART 2018, LNCS 11118, pp. 371–380, 2018.
https://doi.org/10.1007/978-3-030-01168-0_34

characteristics of NR utilizes a very wide spectral range from 1 GHz to 100 GHz. For this it basically considers a beamforming based system as well as scalable numerology. Beamforming can be applied to all signals and data transmitted to each user equipment (UE). In particular, unlike LTE, which is a single-beam-based system, NR is characterized by considering transmission using multiple beams. Accordingly, beam control procedures for setting control signals and beams used for data transmission are introduced. One of the other features is that it supports front-loaded demodulation reference signal (DM-RS) for fast decoding processing time. When control symbols occupy two or three symbols, the front-loaded DM-RS symbol can be located in the 3-rd or 4-th symbol in a slot. In addition, additional DM-RS symbols in a slot can be allocated for coping with the high Doppler effect.

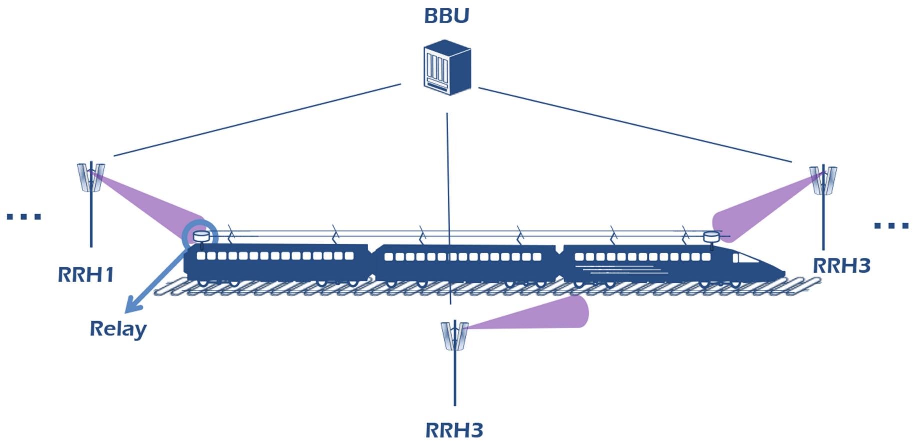

Fig. 1. Linear cell layout for a HST scenario

On the other hand, there are high-speed train (HST) scenarios as one of various service scenarios of 5G mobile communication [2–4, 11]. [2–4] define two scenarios for HST. One is that transmission reception point (TRP) is directly linked with UE in below 6 GHz carrier frequency and the other is that TRP is linked with UE by the relay node in above 6 GHz carrier frequency. [11] defines a HST scenario connected in non-terrestrial networks (NTN) such as high altitude platforms (HAPs). In these scenarios the UE speed is considered up to 500 km/h. In addition, the line of sight (LOS) channel can be dominated. This is because the considered network layout for HST is generally a rural environment and the TRP is located very close to the HST. [2–4] take into account CDL/TDL-D and CDL/TDL-E channels for simulation evaluation parameters in above 6 GHz environment. These channels are constructed to represent the LOS property. In addition, the LOS probability is about 78–99.8% in NTN channel modeling [12].

When DM-RS mapping in NR is applied for channel estimation in HST scenarios, the Doppler effect for high speed may be ignored by using additional

DM-RS symbols with large subcarrier spacing. In the case of LOS channels, however, there may be unnecessary DM-RS resources for spectral efficiency. In other words, the low DM-RS density in the frequency domain can be considered. In this paper, we evaluate the performance using DM-RS of NR in a HST scenario and analyze whether it satisfies the requirement of HST in ITU-R. In addition, we take into account the low density DM-RS mapping design for LOS channel with performance comparison.

2 DM-RS Mapping in a HST Scenario

2.1 Requirements and Layout Configuration

Figure 1 shows linear cell layout configuration for high speed vehicular mobility at 500 km/h under rural-eMBB test environment [3]. In the figure a base station consists of 1 base-band unit (BBU) and 3 remote radio heads (RRHs). 3 RRHs in a cell are connected to 1 BBU. In this configuration one of requirements of HST in ITU-R is spectral efficiency. The spectral efficiency at 500 km/h mobility should satisfy 0.45 b/s/Hz [2]. Various parameters such as channel estimation and phase noise impact can be considered for performance evaluation. As mentioned above, we focus on DM-RS mapping for channel estimation. Phase noise is typically associated with phase tracking (PT)-RS in various reference signals of NR.

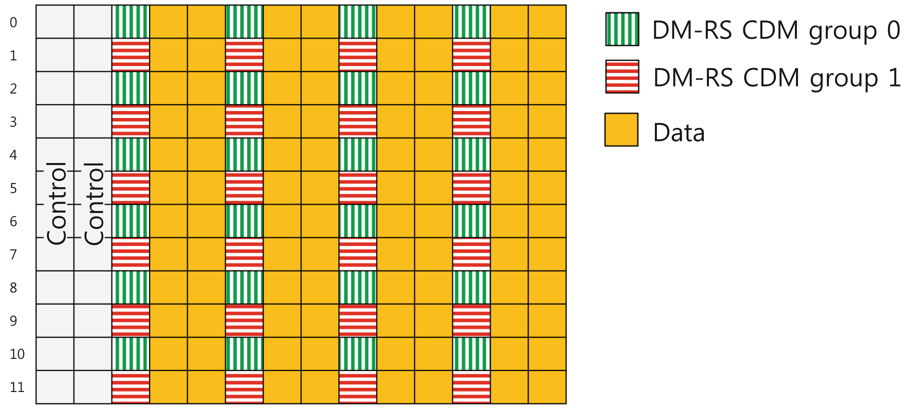

Fig. 2. DM-RS mapping for configuration type 1 in NR

2.2 DM-RS Mapping in NR

The DM-RS sequence at the p-th port for the k-th subcarrier and the l-th symbol for physical downlink shared channel (PDSCH) in NR can be written as follows [5]:

$$a_{k,l}^{(p)} = \beta \cdot w_f(k') \cdot w_t(l') \cdot r(2n + k') \tag{1}$$

where

$$k = \begin{cases} 4n + 2k' + \Delta & \text{Configuration type 1} \\ 6n + k' + \Delta & \text{Configuration type 2} \end{cases}$$
$$k' = 0,\ 1 \qquad (2)$$
$$l = \bar{l} + l'$$
$$n = 0,\ 1,\ \ldots$$

β is power constant and $r(n)$ is the pseudo-random sequence. $w_f(k')$, $w_t(l')$, and Δ are sequence values with cyclic shift of code division multiplexing (CDM) group for distinguishing channel per port. The values are listed in Tables 7.4.1.1.2-1 and 7.4.1.1.2-2 of [5]. The parameter l in (1) is associated with the position of DM-RS symbols in the time domain and the number of DM-RS symbols in a slot can be increased up to 4 in accordance with UE mobility. The values of $\bar{l}$ and l' for l in (2) are given in Tables 7.4.1.1.2-3, 4, and 5 of [5]. There are two kinds of mapping methods according to configuration types. The maximum number of ports in a DM-RS symbol is 4 for configuration type 1 and 6 for configuration type 2. Figure 2 shows an example of DM-RS mapping of configuration type 1 for a resource block (RB) in a slot. The number of subcarriers in the RB is 12. 1 front-loaded DM-RS symbol and 3 additional DM-RS symbols are allocated for coping with high Doppler effect. The parameter k is related to subcarrier mapping in the frequency domain. Based on (1) DM-RS resources in the frequency domain are mapped to all subcarriers allocated per port in each DM-RS symbol.

2.3 DM-RS Mapping for LOS Channel

As mentioned above, assigning DM-RS resources to all subcarriers on the frequency domain for channel estimation may be inefficient in the LOS channel. This is because coherence bandwidth is large. Thus low density DM-RS mapping in the frequency domain can be taken into account. There are various methods for low density DM-RS mapping based on (1). One of several methods is that the RB included in DM-RS subcarriers is allocated per specific RB interval. Based on DM-RS mapping in NR, this method has less influence on the specification than other methods and can be easily applied. In this case physical resource block group (PRG) should be considered when determining a specific RB interval. The PRG consists of consecutive RBs and the PRG size can be equal to one of the values among {2, 4, allocated total RBs} [8]. A precoder is applied per PRG. Since different precoders per PRG are applied to DM-RS, DM-RS in a particular PRG cannot be used for channel estimation for data demodulation in another PRG. Thus DM-RS with a specific RB interval should be included for each PRG. For applying this DM-RS mapping n of (2) can be substituted as follows:

$$\begin{aligned} &k = \begin{cases} 4n + 2k' + \Delta & \text{Configuration type 1} \\ 6n + k' + \Delta & \text{Configuration type 2} \end{cases} \\ &k' = 0,\ 1 \\ &l = \bar{l} + l' \\ &n = S_C \cdot (D_I - 1) \cdot u + v \\ &u = 0,\ 1,\ \ldots, \\ &v = \begin{cases} 0,\ 1,\ 2 & \text{Configuration type 1} \\ 0,\ 1 & \text{Configuration type 2} \end{cases} \end{aligned} \quad (3)$$

where S_C is the number of subcarriers in a RB. D_I is the interval of the RB included in DM-RS symbols. $D_I = i$ means that DM-RS subcarriers are included per i RBs. n is reset per PRG. When D_I is 1, the DM-RS mapping is same with (2). Figure 3 shows an example of DM-RS mapping of configuration type 1 with $D_I = 2$ for a PRG in a slot. As mentioned above, this method can be flexibly applied by adjusting D_I according to the channel environment while having little influence on the current NR standard. It can be applied by adding a radio resource control (RRC) parameter in [10] or associating with downlink control information (DCI) of PRG size in [6].

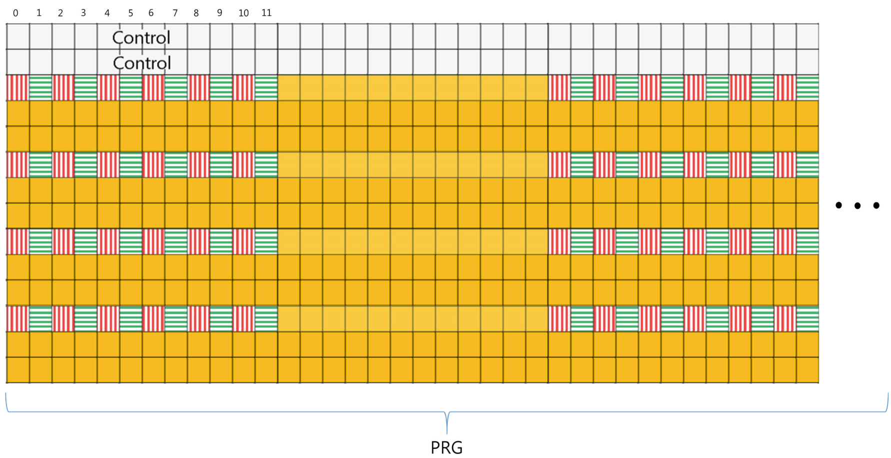

Fig. 3. DM-RS mapping for $D_I = 2$

On the other hand, as D_I becomes larger, channel estimation error may increase due to the decrease of DM-RS resources for channel estimation. On the contrary, one of two benefits for reduced DM-RS resources can be obtained. One can increase the data rate by sending more data to increased data resources. And the other can achieve a coding gain by reducing the coding rate with increased parity bits. For this DM-RS overhead and coding rate are analyzed. The ratio between DM-RS and data subcarriers for D_I can be derived as follows:

$$\mathrm{OH}_{\mathrm{DM-RS}} = \frac{R_S \cdot \left({}^{D_F}/_{D_I}\right)}{D_S \cdot D_F + R_S \cdot D_F \cdot \left(1 - {}^{1}/_{D_I}\right)} \tag{4}$$

where D_S, R_S, and D_F are the number of data symbols in a slot, the number of DM-RS symbols in a slot, and the number of allocated subcarriers in a symbol for data transmission, respectively. When D_I is 1, the number of allocated DM-RS subcarriers per symbol for R_S symbols is same as D_F. The effective coding rate can be written as follows:

$$\mathrm{C}_{\mathrm{eR}} = \frac{\mathrm{TBS}}{Q_M \cdot \left\{D_S \cdot D_F + R_S \cdot D_F \cdot \left(1 - {}^{1}/_{D_I}\right)\right\}} \tag{5}$$

where TBS is transport block size and Q_M denotes modulation order. TBS is determined by the number of allocated data symbols, control symbols, DM-RS symbols, modulation order, and so on [8].

3 Performance Analysis

Simulation parameters for performance evaluation with DM-RS mapping are listed in Table 1, which are referred by [3,4]. In the table, M, N, P, M_g, and N_g are the number of antenna elements with the same polarization in each column on

Table 1. Simulation parameters

Carrier frequency	30 GHz
Subcarrier spacing	120 kHz
Channel bandwidth	80 MHz
TXRU mapping to antenna elements	One TXRU per panel per polarization
BS/Relay antenna configurations	Unidirectional beam ($d_H = d_V = 0.5$) (M, N, P, M_g, N_g) = (8, 8, 2, 1, 1)
Codebook	Type 1 single panel
MCS	QPSK, 0.51
Channel coding	LDPC
Channel model	CDL-D with DS = 10 ns K-factor = 7 dB angle spread: 5 (ASD), 5 (ASA), 1 (ZSA), 1 (ZSD)
UE speed	500 km/h
Channel estimation, Data equalization	MMSE

each antenna panel, the number of columns on each antenna panel, the number of polarization on each antenna panel, the number of panels in a column, and the number of panels in a row, respectively. d_V and d_H denote the spacing in the vertical direction and the spacing of horizontal direction of antenna elements, respectively. BS and relay antenna element radiation patterns are same as Table A.2.1-10 in [4]. The applied beamforming scheme is the combination of analog beamforming and digital beamforming. The best beam pair among the limited set of DFT beams is selected for the decision of analog beam. The DFT beam candidate in this beam selection method is generated according to the uniform vertical and horizontal angular distribution shown as follows:

$$\theta_i = \frac{\pi}{rN_a}, \quad \text{for} \quad i = 1, \cdots, rN_a \tag{6}$$

where $r = 1$ (which is analogous to oversampling factor of 1), N_a denotes the number of vertical/horizontal antennas (M or N). Beam selection is based on the criteria of maximizing receive power after beamforming. In addition, we apply precoder cycling per PRG with type 1 single panel codebook for digital beamforming. The size of PRG is 4 RB. 8 RB is allocated for data transmission. In a slot, we assume that 8, 4, and 2 OFDM symbols are respectively allocated for data transmission of PDSCH, DM-RS for channel estimation, and control transmission of physical downlink control channel (PDCCH). The slot length is

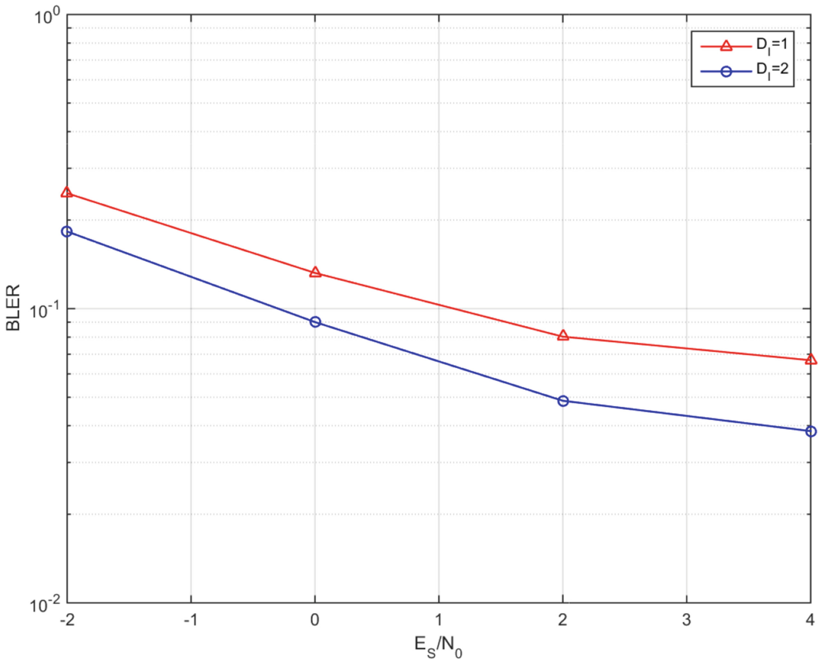

Fig. 4. BLER according to E_S/N_0

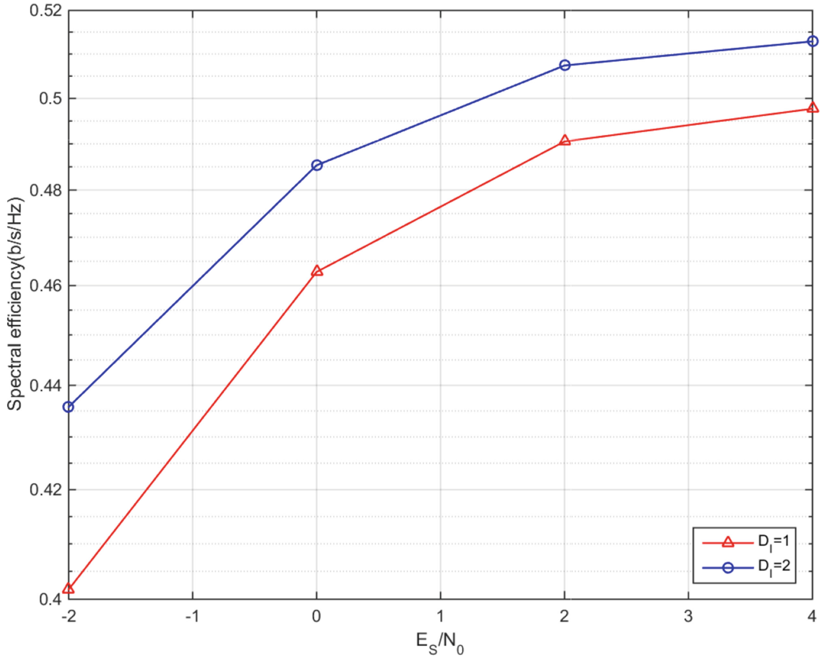

Fig. 5. Spectral efficiency according to E_S/N_0

0.125 ms for 120 kHz subcarrier spacing. Based on [8], TBS is 768. The CDL-D with delay spread (DS)=10 ns is used [13]. K-factor is 7 dB and the parameter set for scaling angle spread is set to 5 (azimuth angle spread of departure (ASD)), 5 (azimuth angle spread of arrival (ASA)), 1 (zenith angle spread of arrival (ZSA)), and 1 (zenith angle spread of departure (ZSD)). Zenith angle Of Departure (ZoD) and Zenith angle Of Arrival (ZoA) for cluster #1 are fixed at 90°.

Figure 4 shows block error rate (BLER) performances in accordance with E_S/N_0. E_S and N_0 denote the power of modulation symbol and the power of AWGN. When D_I is 1, the ratio of DM-RS over data subcarriers is 0.5 based on (4) with simulation parameters. In the case of $D_I = 2$, the ratio of DM-RS over data subcarriers is 0.2. In the case of $D_I = 2$, therefore, DM-RS overhead is reduced compared with $D_I = 1$. However, this leads to the loss of channel estimation accuracy. In addition, TBS for $D_I = 1$ and 2 is 768 according to [8] with simulation parameters. Then coding rates for $D_I = 1$ and 2 are 0.5 and 0.4, respectively, based on 5. Thus the relative coding gain is obtained for $D_I = 2$, compared with $D_I = 1$. As mentioned in Sect. 2.3, the tradeoff between channel estimation error and coding gain is existed. Figure 4 shows that coding gain is more profitable than channel estimation error. $D_I = 2$ satisfies 10% BLER at $E_S/N_0 = -0.3$ dB while $D_I = 1$ requires $E_S/N_0 = 1.1$ dB for 10% BLER. Thus the performance gain is about 1.4 dB for $D_I = 2$. This is because frequency selectivity of CDL-D channel is low and the channel estimation error in accordance with the increase of D_I can be ignored.

Figure 5 shows the spectral efficiency according to E_S/N_0. The spectral efficiency can be derived as follows:

$$\mathrm{SE} = \frac{\mathrm{TBS} \cdot (1 - \mathrm{BLER})}{D_F \cdot S_F \cdot S_L} \tag{7}$$

where S_F denotes the subcarrier spacing and S_L is the slot length. Since the requirement of spectral efficiency at 500 km/h mobility is 0.45 b/s/Hz in the HST scenario, the performances for $D_I = 1$ and 2 satisfy the requirement at $E_S/N_0 = -0.4$ dB and -1.5 dB, respectively. The performance gain for $D_I = 2$ compared with $D_I = 1$ is about 1 dB for 0.45 b/s/Hz. In addition, the average spectral efficiency is increased about 4% for $D_I = 2$.

4 Conclusions

In this paper, we analyze the performance of channel estimation for wireless channels with high mobility and frequency flat characteristics in HST scenarios. It is evaluated whether the application of DM-RS in NR meets the requirement of HST in ITU-R. In addition, we analyze performances for a efficient DM-RS mapping on the LOS channel. Performance analysis shows that the spectral efficiency of HST in ITU-R is satisfied by using DM-RS in NR. And, the efficient DM-RS mapping can obtain about 1 dB E_S/N_0 gain and 4% spectral efficiency gain, compared with DM-RS in NR. The efficient DM-RS mapping can be considered in the NTN environment with a large flat fading characteristic.

Future work is performance analysis considering phase noise and retransmission in HST scenarios. It is also necessary to analyze performances for below 6 GHz carrier frequency.

References

1. Recommendation ITU-R M.2083: IMT Vision - Framework and overall objectives of the future development of IMT for 2020 and beyond, September 2015
2. ITU-R WP5D: Minimum requirements related to technical performance for IMT-2020 radio interface(s), February 2017
3. ITU-R WP5D: Guidelines for evaluation of radio interface technologies for IMT-2020, June 2017
4. 3GPP TR 38.802 V14.2.0: Study on New Radio Access Technology Physical Layer Aspects (Release 14), September 2017
5. 3GPP TS 38.211 V15.1.0: NR; Physical channels and modulation (Release 15), March 2018
6. 3GPP TS 38.212 V15.1.1: NR; Multiplexing and channel coding (Release 15), April 2018
7. 3GPP TS 38.213 V15.1.0: NR; Physical layer procedures for control (Release 15), March 2018

8. 3GPP TS 38.214 V15.1.0: NR; Physical layer procedures for data (Release 15), March 2018
9. 3GPP TS 38.321 V15.1.0: NR; Medium Access Control (MAC) protocol specification (Release 15), March 2018
10. 3GPP TS 38.331 V15.1.0: NR; Radio Resource Control (RRC) protocol specification (Release 15), March 2018
11. 3GPP TR 38.811 V0.4.0: Study on New Radio (NR) to support non terrestrial networks (Release 15), March 2018
12. 3GPP TSG RAN WG1 Meeting #92bis: RAN1 Chairman′s Notes, April 2018
13. 3GPP TR 38.900 V14.3.1: Study on channel model for frequency spectrum above 6 GHz (Release 14), July 2017